

Identification of Bouc-Wen hysteretic parameters based on enhanced response sensitivity approach

Li Wang, Zhong-Rong Lu*

Department of applied mechanics and engineering, Sun Yat-sen University, Guangzhou, 510006, P.R. China

E-mail: wangli75@mail.sysu.edu.cn (Li Wang), lvzhr@mail.sysu.edu.cn (Zhong-Rong Lu)

Abstract. This paper aims to identify parameters of Bouc-Wen hysteretic model using time-domain measured data. It follows a general inverse identification procedure, that is, identifying model parameters is treated as an optimization problem with the nonlinear least squares objective function. Then, the enhanced response sensitivity approach, which has been shown convergent and proper for such kind of problems, is adopted to solve the optimization problem. Numerical tests are undertaken to verify the proposed identification approach.

1. Introduction

The hysteretic behavior is frequently observed in many physical systems [1, 2], such as mechanical systems, structural dampers, oscillatory circuits and so on. Mathematically, hysteresis is characterized as a special type of memory-based relation between the input and the output, that is, the output at a given time instant depends not only on the instantaneous input but also on its past history. Various mathematical models [1, 3–5], including Preisach, Ishlinskii, Bouc-Wen models, have been proposed to describe the hysteretic behavior. In this paper, the focus is on the Bouc-Wen model since it can represent a wide variety of softening/hardening, smoothing-varying/nearly-bilinear hysteretic behavior [6, 7].

Identifying the Bouc-Wen hysteretic parameters is an important and nontrivial task in practical application due to the inherent nonlinearity and memory nature. Over the years, two main kinds of identification methods have been developed. On the one hand, introducing the time discretization and treating the parameters as state variables, the problem becomes a typical discrete state equation and then, parameters are obtained through state estimate using the extended/unscented Kalman filter [8–10] or the wavelet multiresolution analysis [11]. The whole procedure is very simple, however, in order to make the discrete state equation well approximate the original continuous problem, the sampling time step should be small enough. What's worse, the extended/unscented Kalman filter is not an unbiased estimator for such strongly nonlinear problems and in wavelet analysis, the exponential parameter of the Bouc-Wen model should be known *a priori*.

On the other hand, identification of the hysteretic parameters from the measured data belongs to a class of inverse problem and is typically formulated as an optimization problem. The objective function is often established as least squares of the error between the measured data and the derived data and then, actual model parameters should minimize the objective function.



Different kinds of the measured data have led to different identification procedures. Ni, Ko and Wong [12] proposed to use the frequency-domain displacement data from periodic vibration experiment and then, the Levenberg-Marquardt algorithm was adopted to solve the nonlinear least squares optimization problem. However, getting the frequency-domain data of nonlinear dynamic systems is not so straightforward as of linear systems and considerable efforts should be taken for large amount of experimental frequency-domain data. In contrast, the time-domain data is much more easily accessed. Yar and Hammond [7] used the displacement data as well as the restoring force data in time domain to get the parameters. With both displacements and restoring forces obtained, the hysteretic loop graph can be directly plotted and then, parameters are easily derived from the graph. Sues, Roberts and Loh *et al* [13–15] identified the parameters using the time-domain data through a multi-stage estimate scheme. Though satisfactory accuracy as well as convergence was gained, the multi-stage approach is usually time-consuming.

In the present work, the enhanced response sensitivity approach [16–18] which has been widely used in structural damage identification is applied to estimate the Bouc-Wen hysteretic parameters. There are several remarkable features. Firstly, it is within the framework of the least squares optimization and therefore, there is no strict constraint on sampling time step. Secondly, the easily available time-domain data is adopted and arbitrarily single kind or combinatory of the data—the acceleration, the velocity, the displacement or even the restoring force can be used to identify the parameters. Thirdly, the proposed approach can be easily extended to parameter identification of other hysteretic models.

2. Problem statement

2.1. Bouc-Wen hysteretic model

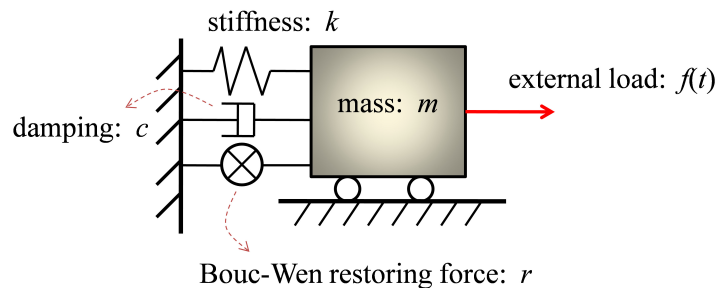


Figure 1. SDOF system with Bouc-Wen hysteresis

Consider a single degree-of-freedom (SDOF) system with the Bouc-Wen hysteretic/restoring force (see Figure 1). The governing equation for motion of the mass is given by

$$\begin{cases} m\ddot{x} + c\dot{x} + kx + r = f(t), t \geq 0 \\ x(0) = x_0, \dot{x}(0) = \dot{x}_0 \end{cases} \quad (1)$$

where x is the displacement, x_0, \dot{x}_0 are initial displacement and velocity of the system and m, c, k, r are respective mass, damping, stiffness and restoring force of the system as shown in Figure 1. In case of the Bouc-Wen hysteretic model, the restoring force r with initial value $r(0) = r_0$ pertains to the following equation [19, 20],

$$\dot{r} = \frac{1}{\eta} [A\dot{x} - \nu(\beta r|r|^{n-1}|\dot{x}| + \gamma|r|^n\dot{x})] \quad (2)$$

where $\eta, A, \nu, \beta, \gamma$ and n are design parameters for the hysteretic behavior. In order to render the parameters identifiable and without loss of generality, the parameters η, ν , which are typically used to control degrading and pinching behavior [10], respectively, are both set to unity herein. The exponential parameter verifies $n \geq 1$ and in order to fulfill the thermodynamic admissibility [20], another constraint $|\gamma| \leq \beta$ should be enforced. In this paper, the linear system parameters m, c, k as well as the Bouc-Wen hysteretic parameters A, β, γ, n are to be identified and the admissible space for all parameters are set to be

$$\mathcal{A} = \{\boldsymbol{\alpha} := (1/m, c/m, k/m, A, \beta, \gamma, n) : 1/m > 0, c/m \geq 0, k/m \geq 0, A > 0, |\gamma| \leq \beta, n \geq 1\}. \quad (3)$$

For practical computation, the problem (1) and (2) is reformulated as

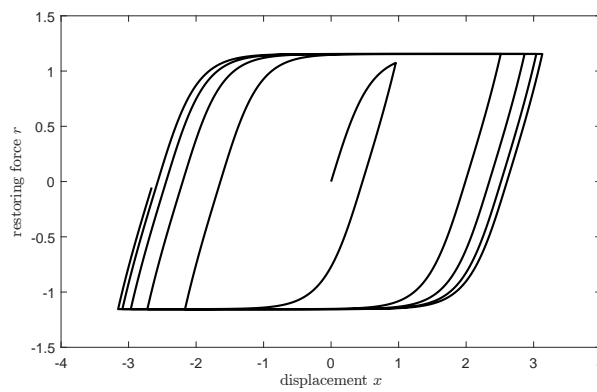


Figure 2. Graph of Bouc-Wen hysteretic loop with parameters $A = 2, \beta = 1, \gamma = 0.5, n = 2$

$$\dot{\boldsymbol{x}} = \boldsymbol{F}(\boldsymbol{x}, \boldsymbol{\alpha}, t) \Leftrightarrow \begin{cases} \dot{x}_1 = x_2 \\ \dot{x}_2 = \alpha_1(f(t) - x_3) - \alpha_2 x_2 - \alpha_3 x_1 \\ \dot{x}_3 = \alpha_4 x_2 - (\alpha_5 x_3 |x_3|^{\alpha_7 - 1} |x_2| + \alpha_6 |x_3|^{\alpha_7} x_2) \end{cases} \quad (4)$$

where $\boldsymbol{x} = [x; y; r]$ and from here on, v_k denotes the k th element of the vector \boldsymbol{v} . Then, given parameters $\boldsymbol{\alpha} \in \mathcal{A}$ of the system, the displacement x , the velocity $\dot{x} = y$, the acceleration $\ddot{x} = \dot{y}$ and the restoring force r of the forward problem are solved from (4) by the Runge-Kutta methods, for which one can refer to the `ode45` function of MATLAB for details. To visual, the hysteretic loop graph under parameters $m = 1, c = 0.2, k = 1, A = 2, \beta = 1, \gamma = 0.5, n = 2$ and loads $f(t) = 2 \cos(t)$ for $t \in [0, 30]$ is shown in Figure 2.

2.2. Inverse problem

Now, assume that some measured data at the time points $t_1 < t_2 < \dots < t_l$ has been obtained, which is designated as a column vector $\hat{\boldsymbol{R}} = [\hat{R}_1; \dots; \hat{R}_l]$ with $\hat{R}_j := \hat{R}(t_j)$ and then, the parameters are to be identified from the data; this forms a typical inverse identification problem. Practically, the measured quantity R can be one or more of the four quantities—the displacement x , the velocity \dot{x} , the acceleration \ddot{x} and the restoring force r and for convenience purpose, it is designated that $R = \mathcal{L}\boldsymbol{x}$ with \mathcal{L} a linear operator, e.g., $\mathcal{L} = [1, 0, 0]$ for $R = x$ and $\mathcal{L} = [0, \frac{d}{dt}, 0]$ for $R = \dot{x}$. Special attention should be paid to the case when only the restoring force r is measured since then the parameters $am, ac, ak, aA, a\beta, a\gamma, n$ can lead to the same restoring force solution for all positive constants $a > 0$. Thus, when only the restoring force r is measured, one shall additional set, for instance, the mass to be known and then, other parameters are well identifiable.

Mathematically, one can deduce from the forward problem (4) that the measured quantity at the time points $t_1 < t_2 < \dots < t_l$ is an implicit function of the parameters and therefore, is expressed as $\mathbf{R}(\boldsymbol{\alpha}) := [R(\boldsymbol{\alpha}, t_1); \dots; R(\boldsymbol{\alpha}, t_l)]$. As usual, the inverse identification procedure can be formulated as: find the actual parameters $\boldsymbol{\alpha}^* \in \mathcal{A}$ such that the objective function $g(\boldsymbol{\alpha})$ —defined as the weighted least squares of the error between the measured data $\hat{\mathbf{R}}$ and the derived data $\mathbf{R}(\boldsymbol{\alpha})$ —is minimized, or, more precisely,

$$\boldsymbol{\alpha}^* = \arg \min_{\boldsymbol{\alpha} \in \mathcal{A}} \left\{ g(\boldsymbol{\alpha}) := \|\hat{\mathbf{R}} - \mathbf{R}(\boldsymbol{\alpha})\|_{\mathbf{W}}^2 \right\} \quad (5)$$

where \mathbf{W} is a user-defined (positive definite) weight matrix and $\|\mathbf{v}\|_{\mathbf{W}}^2 = \mathbf{v}^T \mathbf{W} \mathbf{v}$. Under the above setting, identifying the parameters has become an strongly nonlinear optimization problem. In what follows, how to efficiently and robustly get the minimizer of the objective function $g(\boldsymbol{\alpha})$ by an enhanced response sensitivity approach is elaborated.

3. Enhanced response sensitivity for parameter identification

Usually, $\mathbf{R}(\boldsymbol{\alpha})$ is a nonlinear function of $\boldsymbol{\alpha}$ and therefore, the objective function $g(\boldsymbol{\alpha})$ is in the nonlinear least squares form. For such a nonlinear least-squares optimization problem (5), iterative methods should be used for which the key ingredient is to determine an update $\Delta \boldsymbol{\alpha}$ from a given $\bar{\boldsymbol{\alpha}}$ so that $g(\bar{\boldsymbol{\alpha}} + \Delta \boldsymbol{\alpha})$ becomes as small as possible. The Newton method is costly and improper [18] for such a problem. A simple yet feasible strategy is to linearize $\hat{\mathbf{R}} - \mathbf{R}(\boldsymbol{\alpha})$ at $\bar{\boldsymbol{\alpha}}$ [18, 21], i.e.,

$$\hat{\mathbf{R}} - \mathbf{R}(\boldsymbol{\alpha}) = \Delta \mathbf{R}(\bar{\boldsymbol{\alpha}}) - \mathbf{S}(\bar{\boldsymbol{\alpha}}) \Delta \boldsymbol{\alpha}; \Delta \mathbf{R}(\bar{\boldsymbol{\alpha}}) := \hat{\mathbf{R}} - \mathbf{R}(\bar{\boldsymbol{\alpha}}), \mathbf{S}(\bar{\boldsymbol{\alpha}}) = \nabla_{\boldsymbol{\alpha}} \mathbf{R}(\bar{\boldsymbol{\alpha}}), \Delta \boldsymbol{\alpha} = \boldsymbol{\alpha} - \bar{\boldsymbol{\alpha}}. \quad (6)$$

Specifically, the key matrix $\mathbf{S}(\boldsymbol{\alpha})$ is computed as

$$\mathbf{S}(\boldsymbol{\alpha}) = [\nabla_{\boldsymbol{\alpha}} R(\boldsymbol{\alpha}, t_1); \dots; \nabla_{\boldsymbol{\alpha}} R(\boldsymbol{\alpha}, t_l)]; \nabla_{\boldsymbol{\alpha}} R(\boldsymbol{\alpha}, t_k) = \mathcal{L} \nabla_{\boldsymbol{\alpha}} \mathbf{x}(\boldsymbol{\alpha}, t_k). \quad (7)$$

Note that the key term $\nabla_{\boldsymbol{\alpha}} \mathbf{x}$ is just the (first-order) sensitivity of the response \mathbf{x} to the parameters $\boldsymbol{\alpha}$ and this initiates the name '*response sensitivity approach*'. Obviously, $\nabla_{\boldsymbol{\alpha}} \mathbf{x}$ is time-dependent and pertains to the following ordinary differential equation by applying the differential chain rule to (4),

$$\frac{d(\nabla_{\boldsymbol{\alpha}} \mathbf{x})}{dt} = \nabla_{\mathbf{x}} \mathbf{F}(\mathbf{x}, \boldsymbol{\alpha}, t) \cdot \nabla_{\boldsymbol{\alpha}} \mathbf{x} + \nabla_{\boldsymbol{\alpha}} \mathbf{F}(\mathbf{x}, \boldsymbol{\alpha}, t). \quad (8)$$

For the SDOF system (4) with Bouc-Wen hysteresis, there are

$$\nabla_{\boldsymbol{\alpha}} \mathbf{F}(\mathbf{x}, \boldsymbol{\alpha}, t) = \begin{pmatrix} 0 & 1 & 0 \\ -\alpha_3 & -\alpha_2 & -\alpha_1 \\ 0 & \frac{\partial r}{\partial x_2} & \frac{\partial r}{\partial x_3} \end{pmatrix}; \begin{aligned} \frac{\partial r}{\partial x_2} &:= \alpha_4 - (\alpha_5 x_3 |x_3|^{\alpha_7-1} \text{sgn}(x_2) + \alpha_6 |x_3|^{\alpha_7}) \\ \frac{\partial r}{\partial x_3} &:= -\alpha_7 (\alpha_5 |x_3|^{\alpha_7-1} |x_2| + \alpha_6 |x_3|^{\alpha_7-1} x_2 \text{sgn}(x_3)) \end{aligned} \quad (9)$$

and

$$\begin{aligned} \nabla_{\boldsymbol{\alpha}} \mathbf{F}(\mathbf{x}, \boldsymbol{\alpha}, t) &= \begin{pmatrix} 0 & 0 & 0 & 0 & 0 & 0 & 0 & 0 \\ f(t) - x_3 & -x_2 & -x_1 & 0 & 0 & 0 & 0 & 0 \\ 0 & 0 & 0 & \frac{\partial r}{\partial \alpha_4} & \frac{\partial r}{\partial \alpha_5} & \frac{\partial r}{\partial \alpha_6} & \frac{\partial r}{\partial \alpha_7} & \frac{\partial r}{\partial \alpha_7} \end{pmatrix}; \\ \frac{\partial r}{\partial \alpha_4} &:= x_2, \quad \frac{\partial r}{\partial \alpha_5} := -x_3 |x_3|^{\alpha_7-1} |x_2|, \\ \frac{\partial r}{\partial \alpha_6} &:= -|x_3|^{\alpha_7} x_2, \quad \frac{\partial r}{\partial \alpha_7} := -(\alpha_5 x_3 |x_3|^{\alpha_7-1} |x_2| + \alpha_6 |x_3|^{\alpha_7} x_2) \ln(|x_3| + \epsilon) \end{aligned} \quad (10)$$

where $\text{sgn}(\cdot)$ is the usual sign function and $\epsilon > 0$ is a small positive constant, e.g., $=1.0e-32$, to guarantee the positiveness of $|x_3| + \epsilon$ for $\ln(\cdot)$ function. Combining (4) with (8) and setting $\boldsymbol{\alpha} = \bar{\boldsymbol{\alpha}}$, the response $\mathbf{R}(\bar{\boldsymbol{\alpha}})$ and the response sensitivity $\mathbf{S}(\bar{\boldsymbol{\alpha}})$ are obtainable. Using the linearization (6), an approximate objective function $\hat{g}(\bar{\boldsymbol{\alpha}}, \Delta\boldsymbol{\alpha}) = \|\Delta\mathbf{R}(\bar{\boldsymbol{\alpha}}) - \mathbf{S}(\bar{\boldsymbol{\alpha}})\Delta\boldsymbol{\alpha}\|_{\mathbf{W}}^2$ is obtained which is in the linear least squares form.

The update $\Delta\boldsymbol{\alpha}$, if computed as minimizer of the linear least squares objective function $\hat{g}(\Delta\boldsymbol{\alpha}, \bar{\boldsymbol{\alpha}})$, can be easily and directly obtained; however, $\hat{g}(\Delta\boldsymbol{\alpha}, \bar{\boldsymbol{\alpha}})$ is only an approximation of the original objective function $g(\bar{\boldsymbol{\alpha}} + \Delta\boldsymbol{\alpha})$ through linearization. Note that linearization can give good approximation of the original nonlinear function only when $\Delta\boldsymbol{\alpha} + \bar{\boldsymbol{\alpha}}$ is in the vicinity/trust-region of $\bar{\boldsymbol{\alpha}}$, in other words, the trust-region constraint $\|\Delta\boldsymbol{\alpha}\| \leq \eta$ should hold for some small positive number η . On considering this, a reliable way to get the update $\Delta\boldsymbol{\alpha}$ is clarified: for a certain $\eta > 0$, one has

$$\Delta\boldsymbol{\alpha} = \arg \min_{\delta\boldsymbol{\alpha} \in \mathcal{A} - \bar{\boldsymbol{\alpha}}, \|\delta\boldsymbol{\alpha}\| \leq \eta} \|\Delta\mathbf{R}(\bar{\boldsymbol{\alpha}}) - \mathbf{S}(\bar{\boldsymbol{\alpha}})\delta\boldsymbol{\alpha}\|_{\mathbf{W}}^2. \quad (11)$$

Moreover, to measure how well the linearized version $\hat{g}(\Delta\boldsymbol{\alpha}, \bar{\boldsymbol{\alpha}})$ agrees with the original nonlinear version $g(\bar{\boldsymbol{\alpha}} + \Delta\boldsymbol{\alpha})$, an *agreement indicator* $\rho(\Delta\boldsymbol{\alpha}, \bar{\boldsymbol{\alpha}})$ [18, 21] is introduced,

$$\rho(\Delta\boldsymbol{\alpha}, \bar{\boldsymbol{\alpha}}) := \frac{g(\bar{\boldsymbol{\alpha}}) - g(\bar{\boldsymbol{\alpha}} + \Delta\boldsymbol{\alpha})}{\hat{g}(\mathbf{0}, \bar{\boldsymbol{\alpha}}) - \hat{g}(\Delta\boldsymbol{\alpha}, \bar{\boldsymbol{\alpha}})} = \frac{\|\Delta\mathbf{R}(\bar{\boldsymbol{\alpha}})\|_{\mathbf{W}}^2 - \|\Delta\mathbf{R}(\bar{\boldsymbol{\alpha}} + \Delta\boldsymbol{\alpha})\|_{\mathbf{W}}^2}{\|\Delta\mathbf{R}(\bar{\boldsymbol{\alpha}})\|_{\mathbf{W}}^2 - \|\Delta\mathbf{R}(\bar{\boldsymbol{\alpha}}) - \mathbf{S}(\bar{\boldsymbol{\alpha}})\Delta\boldsymbol{\alpha}\|_{\mathbf{W}}^2}. \quad (12)$$

Good agreement requires $\rho(\Delta\boldsymbol{\alpha}, \bar{\boldsymbol{\alpha}}) \geq \rho_{cr}$ where ρ_{cr} often verifies $\rho_{cr} \in [0.25, 0.75]$. To conclude, in view of (11), different η s result in different updates $\Delta\boldsymbol{\alpha}$ and then, one natural idea is to properly choose the η such that the resulting update verifies the *agreement condition* $\rho(\Delta\boldsymbol{\alpha}, \bar{\boldsymbol{\alpha}}) \geq \rho_{cr}$, which constitutes just the core of trust-region algorithms [21].

In the above derivation, the response sensitivity approach is enhanced with the trust-region restriction, leading to the *enhanced response sensitivity approach*. Nonetheless, solving the inequality-constraint problem (11) is not easy and straightforward at all. Herein, an equivalent but much simpler manner [18] to deal with the trust-region consideration by the Tikhonov regularization is adopted. The procedure reads: find a proper Tikhonov regularization parameter $\lambda > 0$ such that the following update

$$\begin{aligned} \Delta\boldsymbol{\alpha}_\lambda &= \arg \min_{\delta\boldsymbol{\alpha} \in \mathcal{A} - \bar{\boldsymbol{\alpha}}} \{ \|\Delta\mathbf{R}(\bar{\boldsymbol{\alpha}}) - \mathbf{S}(\bar{\boldsymbol{\alpha}})\delta\boldsymbol{\alpha}\|_{\mathbf{W}}^2 + \lambda \|\delta\boldsymbol{\alpha}\|^2 \} \\ &= [\mathbf{S}^T(\bar{\boldsymbol{\alpha}})\mathbf{W}\mathbf{S}(\bar{\boldsymbol{\alpha}}) + \lambda\mathbf{I}]^{-1}\mathbf{S}^T(\bar{\boldsymbol{\alpha}})\mathbf{W}\Delta\mathbf{R}(\bar{\boldsymbol{\alpha}}) \end{aligned} \quad (13)$$

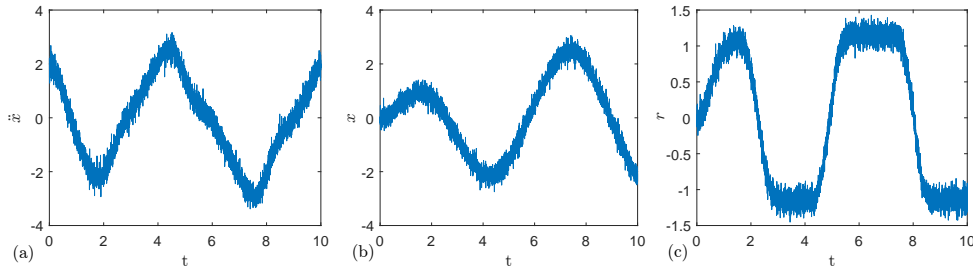
satisfies the agreement condition $\rho(\Delta\boldsymbol{\alpha}_\lambda, \bar{\boldsymbol{\alpha}}) \geq \rho_{cr}$. On the one hand, (13) is still posed to be a linear least squares problem and therefore, is directly solved. On the other hand, the proper Tikhonov regularization parameter $\lambda > 0$ can be simply found as follows: (a) set the regularization parameter $\lambda_L(\bar{\boldsymbol{\alpha}})$ obtained by the L-curve method [22, 23] as the initial regularization parameter, i.e., $\lambda := \lambda_L(\bar{\boldsymbol{\alpha}})$ since such a choice has already been shown to work well for many linear system parameter identification problems [16, 17]; (b) compute the update $\Delta\boldsymbol{\alpha}_\lambda$ as (13); (c) calculate the agreement indicator $\rho(\Delta\boldsymbol{\alpha}_\lambda, \bar{\boldsymbol{\alpha}})$; (d) if the agreement condition is satisfied, terminate the procedure and both the proper λ and the proper update $\Delta\boldsymbol{\alpha}_\lambda$ are obtained, otherwise, increase λ up to a factor $a > 1$, i.e., $\lambda := a\lambda$ and return to step (b). Up till now, a general way to get a proper update from a certain $\bar{\boldsymbol{\alpha}}$ has been presented and based on this, an iterative yet convergent algorithm [18] to get the minimizer of $g(\boldsymbol{\alpha})$ or identify the parameters is naturally established as given in Table 1.

4. Numerical tests

The SDOF system with Bouc-Wen hysteretic force in Figure 1 is elaborately studied herein to testify the proposed parameter identification approach. Actual system parameters are

Table 1. Algorithmic details for enhanced response sensitivity approach

-
- set initial parameters $\boldsymbol{\alpha}_1 \in \mathcal{A}$ and define weight matrix \mathbf{W} ,
 - define error tolerance tol (e.g., $= 10^{-6}$) for convergence criterion,
 - fix the maximum number of iterations $Nmax$ (e.g., $=1000$),
 - fix trust-region parameters $\rho_{cr} \in [0.25, 0.75]$ (e.g., $=0.5$) and $a > 1$ (e.g., $=2$),
 - set the maximum number of steps for trust-region procedure Ntr , (e.g., $=20$),
 - load the measured response data $\hat{\mathbf{R}}$,
 - for $k = 1 : Nmax$
 - solve (4) and (8) to get response $\mathbf{R}(\boldsymbol{\alpha}_k)$ and response sensitivity $\mathbf{S}(\boldsymbol{\alpha}_k)$,
 - compute response change $\Delta\mathbf{R} = \hat{\mathbf{R}} - \mathbf{R}(\boldsymbol{\alpha}_k)$,
 - use L-curve method to get the initial regularization parameter $\lambda_L(\boldsymbol{\alpha}_k)$,
 - for $i = 1 : Ntr$ % Trust-region procedure
 - $\lambda = a^{i-1}\lambda_L(\boldsymbol{\alpha}_k)$,
 - compute the update $\Delta\boldsymbol{\alpha} = [\mathbf{S}^T(\boldsymbol{\alpha}_k)\mathbf{W}\mathbf{S}(\boldsymbol{\alpha}_k) + \lambda\mathbf{I}]^{-1}\mathbf{S}^T(\boldsymbol{\alpha}_k)\mathbf{W}\Delta\mathbf{R}$,
 - if $\boldsymbol{\alpha}_k + \Delta\boldsymbol{\alpha} \notin \mathcal{A}$ continue,
 - solve (4) to get response $\mathbf{R}(\boldsymbol{\alpha}_k + \Delta\boldsymbol{\alpha})$,
 - compute new response change $\Delta\mathbf{R}_{new} = \hat{\mathbf{R}} - \mathbf{R}(\boldsymbol{\alpha}_k + \Delta\boldsymbol{\alpha})$,
 - calculate the agreement indicator $\rho = \frac{\|\Delta\mathbf{R}\|_{\mathbf{W}}^2 - \|\Delta\mathbf{R}_{new}\|_{\mathbf{W}}^2}{\|\Delta\mathbf{R}\|_{\mathbf{W}}^2 - \|\Delta\mathbf{R} - \mathbf{S}(\boldsymbol{\alpha}_k)\Delta\boldsymbol{\alpha}\|_{\mathbf{W}}^2}$,
 - if $\rho \geq \rho_{cr}$ break,
 - end for
 - update stiffness parameters $\boldsymbol{\alpha}_{k+1} = \boldsymbol{\alpha}_k + \Delta\boldsymbol{\alpha}$,
 - if $\|\Delta\boldsymbol{\alpha}\|/\|\boldsymbol{\alpha}_{k+1}\| \leq tol$ break.
 - end for
-

**Figure 3.** Measured data with 5% noise for parameter identification: (a) acceleration \ddot{x} , (b) displacement x and (c) restoring force r

$\boldsymbol{\alpha}^* = (1, 0.2, 1, 2, 1, 0.5, 2)$. A load $f(t) = 2 \cos(t)$ is enforced and the initial states are zero. Herein, the measured data is obtained from numerical simulation over the time domain $[0, 10]$ at the sampling rate of 500Hz and possible measurement noise is added to simulated solution as follows,

$$\hat{\mathbf{d}} = \mathbf{d} + e_{noise}\mathbf{R}_{and}var(\mathbf{d}) \quad (14)$$

where $\mathbf{d} = [d(t_1); \dots; d(t_l)]$, $\hat{\mathbf{d}}$ represents the respective simulated and polluted solutions, e_{noise} is the noise level (e.g., $=5\%$), \mathbf{R}_{and} is a standard normal distribution vector of length l and $var(\mathbf{d})$ is the variance over the time history \mathbf{d} . To visual, the simulated acceleration, displacement and restoring force with measurement noise $e_{noise} = 5\%$ are shown in Figure 3.

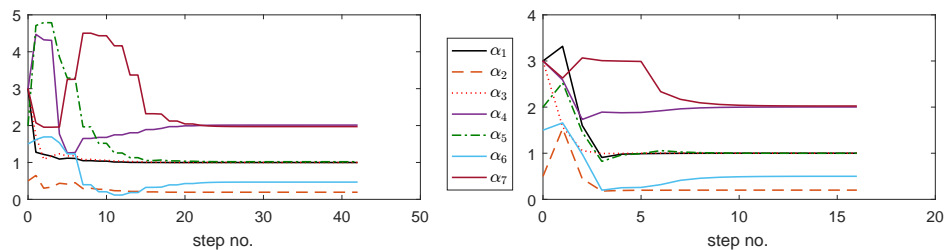
Four identification scenarios as detailed in Table 2 are considered. The algorithm in Table 1 is adopted to derive the parameters from the measured data in all four scenarios, for which,

Table 2. Four identification scenarios for SDOF system with Bouc-Wen hysteresis

scenario	measured quantities	measurement noise
1	acceleration \ddot{x}	0%
2	acceleration \ddot{x}	5%
3	displacement x and restoring force r	0%
4	displacement x and restoring force r	5%

Table 3. Four identification scenarios for SDOF system with Bouc-Wen hysteresis

scenario	identified results
1	(1.0000,0.2000,1.0000,1.9999,1.0001,0.4997,2.0005)
2	(0.9985,0.1933,0.9989,2.0128,1.0202,0.4678,1.9716)
3	(1.0000,0.2000,1.0000,1.9998,1.0002,0.4996,2.0006)
4	(1.0001,0.2003,1.0001,2.0028,0.9990,0.5000,2.0241)

**Figure 4.** Identification procedure for scenario 2 (left) and scenario 4 (right)

the initial parameters are set to be $\alpha_1 = (3, 0.5, 3, 3, 2, 1.5, 3)$, the weight matrix \mathbf{W} equals to identity matrix and other parameters including $tol, Nmax, \rho_{cr}, a, N_{tr}$ take the default values in corresponding brackets of Table 1. Using this algorithm, the parameters can be identified and results are displayed in Table 3. Moreover, to see how the results converge in the iterative procedure, the results in each step of the algorithm are recorded and those for scenarios 2 and 4 are plotted in Figure 4. In case of no noise, either the measured \ddot{x} or the measured x, r can give rise to quite accurate results. While in case of 5% noise, the maximum relative error for measured \ddot{x} (scenario 2) reaches 6% but is only 1.2% for measured x, r (scenario 4) and the results are identified in 42 steps for scenario 2 and 16 steps for scenario 4, this is somehow reasonable since more data often leads to more accurate and faster identification, nevertheless, the identified results are satisfactory.

5. Conclusions

A general way to identify the Bouc-Wen hysteretic parameters has been presented in this paper. It follows the general inverse identification procedure, i.e., transforming the identification to an optimization problem and therefore, can be easily generalized to other hysteretic model parameter identification problems. Then, a recently-proposed enhanced response sensitivity approach is used to solve the nonlinear least squares optimization problem. Numerical tests on four identification scenarios, using single acceleration measurement or displacement and restoring force measurements, with 0% or 5% measurement noise are conducted. All parameters are well identified, highlighting the proposed identification approach.

Acknowledgement

The present investigation was performed under the support of the National Natural Science Foundation of China (No. 11172333) and Guangdong Province Natural Science Foundation (No. 2015A030313126).

References

- [1] Macki JW, Nistri P, Zecca P. Mathematical models for hysteresis. *SIAM Review* 1993, 35(1): 94-123.
- [2] Ismail M, Ikhouane F, Rodellar J. The hysteresis Bouc-Wen model, a survey. *Archives of computational methods in engineering* 2009, 16: 161-188.
- [3] Wen YK. Method of random vibration of hysteretic systems. *ASCE Journal of the Engineering Mechanics Division* 1976, 102: 249-263.
- [4] Belbas SA, Mayergoyz ID. Optimal control of dynamical systems with Preisach hysteresis. *International journal of nonlinear mechanics* 2002, 37: 1351-1361.
- [5] Ikhouane F., Rodellar J. On the hysteretic Bouc-Wen model. Part I: Forced limit cycle characterization. *Nonlinear dynamics* 2005, 42: 63-78.
- [6] Rochdi Y, Giri F, Ikhouane F, Chaoui FZ. Parametric identification of nonlinear hysteretic systems. *Nonlinear dynamics* 2009, 58: 393-404.
- [7] Yar M, Hammond JK. Parameter estimation for hysteretic systems. *Journal of sound and vibration* 1987, 117: 161-172.
- [8] Lin JS, Zhang Y. Nonlinear structural identification using extended Kalman filter. *Computers and structures* 1994, 52: 757-764.
- [9] Corigliano A, Mariani S. Parameter identification in explicit structural dynamics: performance of the extended Kalman filter. *Computer methods in applied mechanics and engineering* 2004, 193: 3807-3835.
- [10] Wu M, Smyth A. Real-time parameter estimation for degrading and pinching hysteretic models. *International journal of nonlinear mechanics* 2008, 43: 822-833.
- [11] Chang CC, Shi Y. Identification of time-varying hysteretic structures using wavelet multiresolution analysis. *International journal of nonlinear mechanics* 2010, 45: 21-34.
- [12] Ni YQ, Ko JM, Wong CW. Identification of nonlinear hysteretic isolators from periodic vibration tests. *Journal of sound and vibration* 1998, 217(4): 737-756.
- [13] Sues RH, Mau ST, Wen YK. Systems identification of degrading hysteretic restoring forces. *ASCE Journal of the Engineering Mechanics* 1988, 114: 833-846.
- [14] Roberts JB, Sadeghi AH. Sequential parameter identification and response of hysteretic oscillators with random excitation. *Structural safety* 1990, 8: 45-68.
- [15] Loh CH, Chung ST. A three-stage identification approach for hysteretic systems. *Earthquake engineering and structural dynamics* 1993, 22: 129-150.
- [16] Lu ZR, Law SS. Features of dynamic response sensitivity and its application in damage detection. *Journal of sound and vibration* 2007, 303: 305-329.
- [17] Fu YZ, Lu ZR, Liu JK. Damage identification in plates using finite element model updating in time domain. *Journal of sound and vibration* 2013, 332: 7018-7032.
- [18] Lu ZR, Wang L. An enhanced response sensitivity approach for structural damage identification: convergence and performance. *International journal for numerical methods in engineering* 2017, DOI: 10.1002/nme.5502.
- [19] Brewick PT, Masri SF. An evaluation of data-driven identification strategies for complex nonlinear dynamic systems. *Nonlinear dynamics* 2016, 85: 1297-1318.
- [20] Erlicher S, Point N. Thermodynamic admissibility of Bouc-Wen type hysteresis models. *Comptes rendus mecanique* 2004, 332: 51-57.
- [21] More JJ. The Levenberg-Marquardt algorithm: implementation and theory. Chapter Numerical analysis, volume 630 of the series *Lecture Notes in Mathematics* 1978, pp: 105-116.
- [22] Hansen PC. Analysis of discrete ill-posed problems by means of the L-curves. *SIAM Review* 1992, 34(4): 561-580.
- [23] Hansen PC. Regularization tools—A matlab package for analysis and solution of discrete ill-posed problem. *Numerical algorithms* 1994, 6(1): 1-35.